INTERNATIONAL JOURNAL FOR NUMERICAL METHODS IN FLUIDS, VOL. 21, 653–665 (1995)

A NUMERICAL STUDY OF FLOW OVER A CONFINED BACKWARD-FACING STEP

I. E. BARTON

Aerospace Engineering Division, Manchester School of Engineering, Oxford Road, Manchester University, Manchester M13 9PL, U.K.

SUMMARY

Numerical solutions using the SIMPLE algorithms for laminar flow over a backward-facing step are presented. Five differencing schemes were used: hybrid; quadratic upwind (QUICK); second-order upwind (SOUD); central-differencing and a novel scheme named second-order upwind biased (SOUBD). The SOUBD scheme is shown to be part of a family of schemes which include the central-differencing, SOUD and QUICK schemes for uniform grids. The results of the backward-facing step problem are presented and are compared with other numerical solutions and experimental data to evaluate the accuracy of the differencing schemes. The accuracy of the differencing schemes was ascertained by using uniform grids of various grid densities. The QUICK, SOUBD and SOUD schemes gave very similar accurate results. The hybrid scheme suffered from excessive diffusion except for the finest grids and the central-differencing scheme only converged for the finest grids.

KEY WORDS: backward-facing step; laminar flow; discretization schemes; second-order upwind differencing

INTRODUCTION

The backward-facing step is one of the most fundamental geometries where laminar separation occurs caused by the sudden change in the geometry. The present study has investigated a classical planar, laminar backward-facing step flow originally studied by Armaly *et al.*[1] The geometry of the problem is shown in Figure 1. The expansion ratio of the inlet channel height, h, to the outlet height is 1:2. The upper boundary layer simplifies computational boundary conditions making the problem readily applicable to numerical procedures. At low Reynolds numbers the flow behaves like an open backward-facing step flow where the flow separates at the step and reattaches further downstream. The reattachment length increases almost linearly with Reynolds number, the slight non-linear trend is caused by the viscous drag along the upper boundary. For higher Reynolds numbers the adverse pressure gradient is strong enough to cause separation along the upper boundary which reattaches further downstream. The upper recirculation region causes the growth of the lower reattachment to be decreased even further this behavior has numerically investigated by Barton.[2] Armaly *et al.*[1] experimentally investigated the problem and also carried out a numerical study, which failed to obtain good agreement with the experimental data because of the inadequate grid resolution. Kim and Moin[3] conducted one of the first numerical studies which gave good agreement with the experimental data of Armaly *et al.*[1] up to $Re = 500$, where the Reynolds number is defined using $2h$ as the length scale and the mean u-velocity at the step as the velocity term. The disagreement between the numerical and experimental results for higher Reynolds numbers is probably caused by the three-dimensional experimental effects. Caruso *et al.*[4] used grid adaption in an attempt to improve numerical results.

CCC 0271–2091/95/080653–13

Received October 1994
Revised February 1995

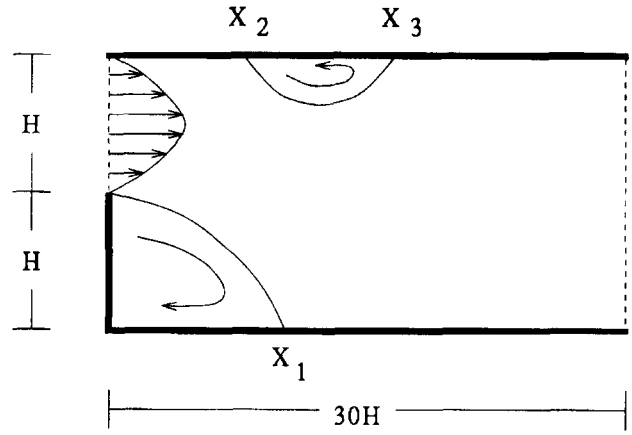

Figure 1. The backward-facing step geometry and recirculation regions for a high Reynolds flow

They found little difference with the predictions of Kim and Moin[3] which used a uniform 101 × 101 grid. Indeed, subsequent numerical studies[5–9] gave very similar predictions with the exception of Orlandi,[10] who found that using a non-uniform grid introduced a strong numerical diffusion effect due to low-order truncation errors.

The present study concentrates on a detailed grid dependency investigation using a variety of differencing schemes. The study mainly uses various uniform computational grids, which is not desirable in terms of computational cost but does have two advantages. First, the work is easily reproducible and second, truncation errors associated with non-uniform grids are avoided.

THE GOVERNING EQUATIONS

The governing equations for planar, incompressible, laminar flow are

$$\frac{\partial \rho u}{\partial x} + \frac{\partial \rho y}{\partial y} = 0, \tag{1}$$

$$\frac{\partial \rho u^2}{\partial x} + \frac{\partial \rho uv}{\partial y} = -\frac{\partial p}{\partial x} + \mu\left(\frac{\partial^2 u}{\partial x^2} + \frac{\partial^2 u}{\partial y^2}\right), \tag{2}$$

$$\frac{\partial \rho uv}{\partial x} + \frac{\partial \rho v^2}{\partial y} = -\frac{\partial p}{\partial y} + \mu\left(\frac{\partial^2 v}{\partial x^2} + \frac{\partial^2 v}{\partial y^2}\right). \tag{3}$$

The variables are non-dimensionalized using the height of the inlet channel, h, the mean velocity u_m, and the pressure coefficient $\frac{1}{2}\rho u_m^2$. The Reynolds number is defined by $Re = 2\rho h u_m/\mu$, where ρ is the density and μ is the viscosity of the flow.

THE BOUNDARY CONDITIONS

Similar to other numerical studies, a fully developed parabola u-velocity profile is prescribed at the inlet. The outlet is a total length of 30 h downstream of the step. The horizontal length of 30 h is sufficiently long enough not to effect the upstream recirculation regions. The outlet boundary conditions assume the outlet diffusion terms are zero. The outlet condition is doubtful although it has been applied to similar studies. No-slip boundary conditions are applied for the wall boundaries.

DISCRETIZATION AND THE COMPUTATIONAL GRID SYSTEM

The governing equations are solved in primitive form (u, v, p), the solution procedure is discussed later. The partial differential equations are discretized on to a staggered computational grid system.[11] The velocities are located on the faces of the cell and the pressure term is located at the centroid of the control volume. Staggering the primitive terms (u, v, p) allows the continuity equation to be integrated over a single control volume and prevents odd-even coupling.[12] A single control volume with adjacent east and west control volumes are shown in Figure 2.

The diffusion terms can be successfully discretized using central-differencing because it is third-order accurate and diffusion dominated solutions have slow spatial variation. The discretization of the convection terms are not as straight-forward, which is shown by integrating a convection term across a control volume (in one dimension):

$$\int \frac{\partial \rho u \phi}{\partial x} \partial x = (\rho u) e \phi_e - (\rho u)_w \phi_w, \tag{4}$$

because the terms ϕ_e and ϕ_w have to be interpolated, using a differencing scheme. The present study uses the following schemes central-difference, quadratic upwind interpolation for convection kinetics (QUICK), second-order upwind bias difference (SOUBD), second-order upwind difference (SOUD) and the hybrid scheme. The former schemes were chosen because they form a family of schemes for uniform grids, this is discussed later. The interpolation assumptions for the various schemes are summarized below for the ϕ_e term.

(i) The central difference scheme:

$$\phi_e = \tfrac{1}{2}(\phi_P + \phi_E). \tag{5}$$

Central differencing is second-order accurate but it tends to fail giving a spatial oscillatory solution for the no-source convection-diffusion equation with fixed boundaries when the grid Peclet number, Pe_G, is greater than two.[13]

$$Pe_G = \frac{\rho u \Delta x}{\Gamma_\phi} \tag{6}$$

In practice, non-oscillatory solutions can be predicted for values of Pe_G greater than two, away from fixed boundaries conditions, for example away from wall boundaries. Nevertheless, the central-differencing scheme is unstable, unlike 'upwind' schemes.

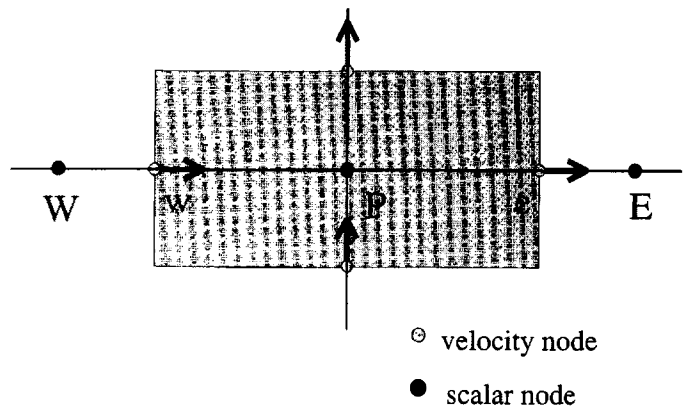

Figure 2. The grid notation for a pole-cell and its adjacent east and west cells

(ii) Quadratic upstream interpolation for convection kinematics (QUICK):
if $Pe_G \geq 0$,

$$\phi_e = \tfrac{1}{2}(\phi_E + \phi_P) - \tfrac{1}{8}(\phi_E - 2\phi_P + \phi_W); \tag{7}$$

if $Pe_G < 0$,

$$\phi_e = \tfrac{1}{2}(\phi_E + \phi_P) = \tfrac{1}{8}(\phi_{EE} - 2\phi_E + \phi_P). \tag{8}$$

The QUICK scheme[14] uses a quadratic fit through the two adjacent nodes and a third upwind node to find the interpolated value. The upwind term gives the scheme greater stability than central-differencing. The scheme has been extensively used in technical studies. The QUICK scheme can converge faster for low Peclet numbers compared with the hybrid scheme but it becomes unstable for high Peclet numbers unless the coefficients are revised in some form. Patel and Markatos[15] used the recommended revision of Pollard and Siu[16] and found the revision reduced the rate of convergence but increased the stability of the scheme.

(iii) Second-order upwind biased difference scheme (SOUBD):
if $Pe_G \geq 0$,

$$\phi_e = \phi_P + \tfrac{1}{4}(\phi_E - \phi_W); \tag{9}$$

if $Pe_G < 0$,

$$\phi_e = \phi_E - \tfrac{1}{4}(\phi_{EE} - \phi_P). \tag{10}$$

The scheme uses the adjacent upwind node and extrapolates to the cell face value similar to the SOUD scheme; unlike the SOUD scheme the gradient is calculated by central-differencing. The SOUBD scheme therefore has greater accuracy than the SOUD scheme, as the third-order truncation error is smaller. The improved accuracy however has the almost inevitable consequence of making the scheme less stable and prone to predict spatial oscillatory solutions.

(iv) Second-order upwind difference scheme (SOUD):
if $Pe_G \geq 0$,

$$\phi_e = \phi_P + \tfrac{1}{2}(\phi_P - \phi_W); \tag{11}$$

if $Pe_G < 0$,

$$\phi_e = \phi_E - \tfrac{1}{2}(\phi_{EE} - \phi_E). \tag{12}$$

The SOUD scheme[17] uses only upwind terms to extrapolate the cell face value and therefore the scheme has excellent stability quantities. In comparison with QUICK, Shyy[18] and Sharif and Busnaina[19] concluded that SOUD is the superior scheme for large grid Peclet numbers where the QUICK scheme tends to predict spatially oscillatory solutions.

There exists a generalized relationship between the QUICK, SOUD and the central differencing schemes for uniform grids.[20] Considering the flow westward, these schemes can be expressed in general terms as

$$U_e = \tfrac{1}{2}(U_E + U_P) - \tfrac{1}{2}q(U_{EE} + U_P - 2U_E), \tag{13}$$

where the parameter q is set to zero to give central differencing, $q = 1/4$ to give QUICK differencing, $q = 1$ to give SOUD differencing. It is straightforward to show that the SOUBD scheme corresponds to the parameter $q = 1/2$.

(v) The hybrid difference scheme:
if $Pe_G > 2$,

$$\phi_e = \phi_P; \tag{14}$$

if $2 \geq Pe_G \geq -2$,

$$\phi_e = \tfrac{1}{2}(\phi_P + \phi_E); \tag{15}$$

if $Pe_G < -2$,

$$\phi_e = \phi_E. \tag{16}$$

The hybrid differencing scheme[21] has the accurate features of central differencing for low Pe_G numbers and switches to the first-order accurate upwind differencing for Pe_G numbers with an absolute value of two or greater. The scheme also ignores the physical viscosity when applying the upwind interpolation. This is a reasonable assumption as the truncation error caused by first-order upwind differencing is likely to be at least the same order of magnitude. The hybrid scheme is stable and robust and has been used extensively in engineering applications.

When the finite-difference approximations are applied to the partial differential equations, they can be expressed as algebraic equations, in the following form:

$$A_P\phi_P = A_N\phi_N + A_E\phi_E + A_S\phi_S + A_W\phi_W + S_A + S_B, \tag{17}$$

where the source term, S_A, contains extra coefficient terms required for schemes such as QUICK, S_B relates to the physical source terms such as the pressure gradient in the case of the momentum equations.

The formulation of the coefficient terms has been discussed elsewhere.[12] The formulation of revised coefficients terms for the central-differencing scheme in one-dimension is briefly discussed to demonstrate the concepts behind Pollard and Siu's revised formulation of the QUICK scheme.[16] Pollard and Siu's revision includes the following conditions: the A coefficients must never become negative; the solution of convection dominated flows should be essentially stable. The derivation is simplified with the definition of the following convection and diffusion terms

$$C_i = \rho u_i, \quad D_i = \Gamma_i/\Delta x. \tag{18}$$

The following coefficients meet the above requirements for central-differencing (in one dimension):

$$A_E = D_e + |\tfrac{1}{2}C_e|, \tag{19}$$

$$A_W = D_w + |\tfrac{1}{2}C_w|, \tag{20}$$

$$A_P = A_E + A_W. \tag{21}$$

If we ignore the source term S_A it is clear that the above coefficients lead to a physically realistic solution if the convection terms dominate, normal coefficient terms with low diffusion terms would lead to unstable solutions.[12] Additional terms are required to make the above algebraic equation physically correct these terms are contained in the source term, S_A, and are explicitly treated to prevent divergence in the matrix solution procedure

$$S_A = -M_e^+ C_e\Phi_E + M_w^- C_w\Phi_W - M_e^- C_e\Phi_P + M_w^+ C_w\Phi_P, \tag{22}$$

where the M coefficients are

$$M_j^{\pm} = \frac{(C_j \pm |C_j|)}{2C_j}, \quad j = e, w. \tag{23}$$

The revision can also be applied to the SOUD and SOUBD schemes. The individual sets of coefficients for central-differencing, QUICK, SOUBD and SOUD are presented in a revised

generalized form

$$A_{N,E} = [D_{n,e} + (\tfrac{1}{2}+q)C_{n,e}, D_{n,e} - (\tfrac{1}{2}+q)C_{n,e} - \tfrac{1}{2}qC_{s,w}, D_{n,e} - (\tfrac{1}{2}+q)C_{n,e}, D_{n,e} + (\tfrac{1}{2}+q)C_{n,e} - \tfrac{1}{2}qC_{s,w}], \tag{24}$$

$$A_{S,W} = [D_{s,w} - (\tfrac{1}{2}+q)C_{s,w}, D_{s,w} + (\tfrac{1}{2}+q)C_{s,w} + \tfrac{1}{2}qC_{n,e}, D_{s,w} + (\tfrac{1}{2}+q)C_{s,w}, D_{s,w} - (\tfrac{1}{2}+q)C_{s,w} + \tfrac{1}{2}qC_{n,e}], \tag{25}$$

$$A_P = A_N + A_E + A_S + A_W. \tag{26}$$

The function $[A, B]$ selects the maximum value

$$S_A = S_A^1 + S_A^2. \tag{27}$$

The source term, S_A, is split into two parts, S_A^1 and S_A^2, the first part corrects upwind terms and the second the pole-coefficient term

$$S_A^1 = -\tfrac{1}{2}q(M_w^+ C_w \Phi_{WW} + M_s^+ C_s \Phi_{SS} - M_e^- C_e \Phi_{EE} - M_n^- C_n \Phi_{NN}) - (1+\tfrac{1}{2}q)(M_e^+ C_e \Phi_E + M_n^+ C_n \Phi_N - M_w^- C_w \Phi_W - M_s^- C_s \Phi_S), \tag{28}$$

$$S_A^2 = \tfrac{1}{2}q(M_e^+ C_e + M_n^+ C_n - M_w^- C_w - M_s^- C_s)\Phi_P + (1+\tfrac{1}{2}q)(M_s^+ C_s + M_w^+ C_w - M_e^- C_e - M_n^- C_n)\Phi_P. \tag{29}$$

In conclusion, the above equations have combined the generalized formulation[20] with the coefficient revision of Pollard and Siu.[16] Clearly, the main advantage of this approach is it simplifies computer coding. The coefficient terms for the hybrid differencing scheme are discussed in Patankar.[12]

THE UNIFORM GRIDS

The present study uses the following uniform grids: a very coarse grid (15 × 8); two coarse grids (30 × 16) and (40 × 20): two medium grids (80 × 40) and (120 × 50); two fine grids (160 × 80) and (200 × 100); and a very fine grid (250 × 128). The terms coarse, medium and fine have been used in the preceding sections as well as the grid labelling of 1 to 8 (grid (1) is the very coarse grid). The very fine grid was only used for the hybrid scheme due to time limitations and because the coarser grids are satisfactory for other differencing schemes.

THE SOLUTION PROCEDURE

The semi-implicit method for pressure linked equations (SIMPLE) methodology is used to solve the governing equations.[12,20,22] The algorithm is briefly described. The Navier–Stokes equations are solved using the current pressure field (which is initially guessed). The continuity equation is expressed in the form of a pressure correction equation and the velocity and pressure fields are then corrected to satisfy continuity equation. The whole procedure is then repeated until the velocity and pressure fields converge.

The SIMPLE methodology uses a pseudo-time step term non-dimensionalized by $\rho\Delta x\Delta y/A_p$. Raithby and Schneider[22] studied a variety of problems and concluded a time step parameter of about four is optimal. Lower time step values lead to slower converging solutions but improves stability. The central-differencing scheme fails to converge for the coarser grids even if the time step parameter is set to extremely low values. The other schemes converge for time step parameters ranging from 0·3 to 4

where the QUICK scheme converges slowly compared with SOUD, and the hybrid scheme converges the most rapidly. The velocity under-relaxation parameters were set to $\alpha_{u,v} = 0{\cdot}7$. The pressure correction under-relaxation parameter was calculated from the following relationship,[22] where E is the time step parameter

$$\alpha_p \approx \frac{1}{1+E}. \tag{30}$$

The solution was assumed to have converged when the maximum absolute relative change between successive iterations was less than 10^{-5} for all velocity and the pressure values and when the fluid residuals have decreased to 10^{-5} of their original value.

The algebraic equations are solved by using a tri-diagonal matrix solution procedure (TDMA). The TDMA procedure is applied in the y-co-ordinate direction and successively sweeps through the computational domain in the x-direction, (the streamwise direction).

THE RESULTS

The changes in reattachment and separation positions from a coarse to fine grid tend to increase with Reynolds number. The hybrid scheme has the highest percentage changes in reattachment and separation positions. This is shown in Table I, which shows the percentage change in the reattachment lengths x_1 for the various schemes from medium to fine grids. The hybrid scheme tends to fail to give reliable results for Reynolds numbers of $Re = 500$ and above. The central differencing scheme fails to converge for $Re = 500$ and above using medium grids so no relative change can be considered. Clearly, for $Re = 500$ and above, a central differencing approach is unstable and the hybrid scheme switches to first-order upwind differencing which proves to be inaccurate. All the other schemes have low percentage changes across the entire range of Reynolds numbers. The values of the reattachment and separation lengths x_1, x_2 and x_3 are determined by interpolation using velocity data at the spatial locations near the reattachment or separation regions.

Estimated grid independent reattachment and separation lengths are calculated by fitting a straight line through the top three or four finest grid results against their average x-co-ordinate mesh Peclet number. The intercept is taken to be the independent result. The estimated grid independent results using the QUICK, SOUBD and SOUD schemes are virtually the same. The estimated grid independent results are used to make comparisons with previous sets of results. A low Reynolds number case, $Re = 300$, is considered in Table II, the table gives the percentage difference from the estimated independent results and the results for the various grids. Table II demonstrates how similar the results are for the QUICK, SOUBD and SOUD schemes, all these schemes give acceptable results for grids (4) to (8). The hybrid scheme gives more disappointing results requiring grid (8) to give similar agreement compared with QUICK, SOUBD and SOUD. The central differencing scheme requires a

Table I. Percentage change in lower reattachment length for various schemes from medium to fine grids

Re	hybrid	central	QUICK	SOUBD	SOUD
50	0·6	0·9	0·1	0·4	0·9
100	1·0	0·4	0·2	0·8	1·1
200	0·7	0·4	0·4	0·6	1·0
300	0·7	0·4	0·2	0·4	0·5
400	1·0	0·6	0·1	0·1	0·2
500	3·1	—	0·1	0·4	1·0
600	8·0	—	0·3	0·7	0·9

Table II. The lower reattachment length x_1 for various grids and (the percentage difference from the estimated grid independent result) for $Re = 300$

grid	hybrid	central	QUICK	SOUBD	SOUD
1	7·99 (11·9)	—	7·74 (8·4)	7·68 (7·6)	7·61 (6·6)
2	7·46 (4·5)	—	7·36 (3·0)	7·40 (3·7)	7·44 (4·2)
3	7·25 (2·0)	—	7·29 (2·1)	7·32 (2·5)	7·34 (2·7)
4	6·97 (2·5)	—	7·15 (0·2)	7·18 (0·5)	7·21 (1·0)
5	7·00 (2·0)	7·11 (0·5)	7·15 (0·1)	7·16 (0·3)	7·17 (0·5)
6	7·02 (1·7)	7·05 (1·6)	7·13 (0·3)	7·15 (0·1)	7·16 (0·1)
7	7·05 (1·3)	7·14 (0·1)	7·15 (0·1)	7·16 (0·2)	7·17 (0·4)
8	7·08 (0·9)				

grid at least as fine as grid (5) to converge. The grid dependency behaviour of the lower reattachment length x_1 is also investigated in Table II. The QUICK, SOUBD and SOUD schemes predict almost parallel results with QUICK predicting the smallest value of x_1. Also, these three schemes predict a large reattachment length for coarse grids converging to a smaller value with grid refinement. The SOUD scheme tends to predict a slightly larger lower reattachment length because of an 'upwind effect'. The position of the maximum u-velocity is slighly higher compared with the QUICK scheme result, this prevents early reattachment. The hybrid scheme tends to predict a large lower reattachment length for coarse grids where the scheme is dominated by numerical diffusion. Initially, the effect of switching to central-differencing causes the lower reattachment length to decrease but the length tends to increase in size as central-differencing becomes more appropriate.

A higher Reynolds number case, $Re = 600$, has an upper recirculation region. The percentage difference between the reattachment and separation length results from their estimated grid independent results are presented in Table III. The most difficult feature to resolve was the separation position x_2, this is because the upper recirculation region is very sensitive, interacting with the lower reattachment length. In Table III all the schemes perform worst for the lower reattachment position compared with the low Reynolds number results. The QUICK, SOUD and SOUBD schemes give acceptable results for all the reattachment and separation lengths for the grids (5) to (8), the QUICK scheme seems to give slightly better agreement than the other schemes. The hybrid scheme fails to give any acceptable results with fairly large percentage differences for even the finest grid. The central-differencing scheme gives good agreement for grid (7), the results are poor for grid (6), convergence cannot be obtained for the coarser grids. In Table III the grid dependency behavior for the reattachment and separation lengths is also investigated. The high Reynolds case, similar to the low Reynolds case, predicts almost parallel results for the QUICK, SOUBD and SOUD schemes. However, the lower reattachment length increases in size with grid refinement, whereas for the low Reynolds number case it decreases. The increase in the lower reattachment length x_1, is caused by the upper recirculation region. The coarse grids tend to predict a large upper recirculation region causing early reattachment for the lower boundary. The SOUD scheme tends to be most affected, predicting the largest upper recirculation regions and thus the smallest lower reattachment lengths.

The estimated grid reattachment and separation lengths are summarized on Figure 3 as well as the experimental data of Armaly *et al.*[1] The present numerical predictions agree satisfactorily with the experimental results up to $Re = 500$, Armaly *et al.*[1] observed three dimensional effects occurred for higher Reynolds numbers which probably explains the deviation. On the same figure the predictions of Guj and Stella[7] are shown, other predictions give similar results. The present predictions have slightly larger x_1 and x_3 values for the higher Reynolds numbers compared with Guj and Stella[7], this suggests that the present results are more accurate as these lengths tend to increase with grid refinement.

Table III(a). The lower reattachment length x_1 for various grids and (the percentage difference from the estimated grid independent result) for $Re = 600$

grid	hybrid	central	QUICK	SOUBD	SOUD
1	14·28 (33·1)	—	8·46 (26·8)	8·52 (26·0)	8·77 (22·4)
2	11·88 (10·7)	—	10·08 (6·5)	9·64 (11·4)	9·11 (17·8)
3	9·24 (16·2)	—	10·41 (2·8)	10·12 (6·0)	9·71 (10·5)
4	8·98 (19·6)	—	10·57 (1·2)	10·60 (1·0)	10·54 (1·5)
5	9·58 (12·1)	—	10·66 (0·4)	10·63 (0·7)	10·57 (1·2)
6	9·41 (8·0)	10·51 (1·8)	10·63 (0·6)	10·72 (0·2)	10·69 (0·2)
7	10·10 (6·3)	10·72 (0·2)	10·67 (0·3)	10·65 (0·5)	10·61 (0·8)
8	10·32 (4·0)				

Table III(b). The separation length x_2 for various grids and (the percentage difference from the estimated grid independent result) for $Re = 600$

grid	hybrid	central	QUICK	SOUBD	SOUD
1	—	—	4·19 (52·7)	5·60 (35·7)	7·54 (15·5)
2	9·60 (10·2)	—	7·65 (13·8)	7·42 (17·4)	6·84 (21·4)
3	6·74 (29·2)	—	8·17 (6·5)	7·94 (9·7)	7·48 (14·0)
4	6·93 (25·7)	—	8·42 (3·3)	8·31 (4·5)	8·09 (6·5)
5	7·50 (16·1)	—	8·59 (1·4)	8·55 (1·8)	8·49 (2·5)
6	7·83 (11·2)	8·52 (2·2)	8·57 (1·3)	8·62 (1·0)	8·62 (1·6)
7	8·03 (8·4)	8·72 (0·1)	8·63 (0·8)	8·61 (1·0)	8·57 (1·0)
8	8·26 (5·4)				

Table III(c). The reattachment length x_3 for various grids and (the percentage difference from the estimated grid independent result) for $Re = 600$

grid	hybrid	central	QUICK	SOUBD	SOUD
1	—	—	11·21 (31·0)	12·68 (21·9)	12·56 (22·7)
2	10·67 (34·3)	—	15·86 (2·2)	15·77 (3·0)	15·76 (3·1)
3	11·49 (29·3)	—	16·11 (0·8)	16·15 (0·6)	16·17 (0·4)
4	13·49 (16·9)	—	16·15 (0·6)	16·18 (0·4)	16·25 (0·1)
5	14·59 (11·3)	—	16·17 (0·4)	16·22 (0·1)	16·29 (0·3)
6	15·11 (7·5)	15·85 (2·5)	16·17 (0·4)	16·18 (0·4)	16·24 (0·03)
7	15·39 (5·5)	16·15 (0·6)	16·21 (0·2)	16·24(0·02)	16·28 (0·2)
8	5·65 (3·8)				

However, the differences could also be caused by slight differences in geometry and inlet conditions.

The u-velocity profiles for the QUICK, SOUBD and SOUD schemes are virtually identical for coarse, medium and fine grids for the entire Reynolds number range. The hybrid scheme however does not produce identical profiles. In the case of $Re = 100$, the coarse grid results have a large u-velocity at $x = 3h$ near the top boundary, compared with the medium and fine grids. For $Re = 300$ the hybrid scheme again predicts a larger u-velocity near the top boundary at $x = 6h$ to $x = 12h$ for the coarse grids in comparison with the medium and fine grid results. In the $Re = 500$ case, the coarse grid results have a larger u-velocity near the top boundary at $x = 9h$ to $x = 15h$ in comparison with the medium and fine grid results.

The grid dependency of the pressure field is considered using the maximum pressure relative to the step corner, non-dimensionalized using the mean inlet u-velocity and inlet density. For low Reynolds

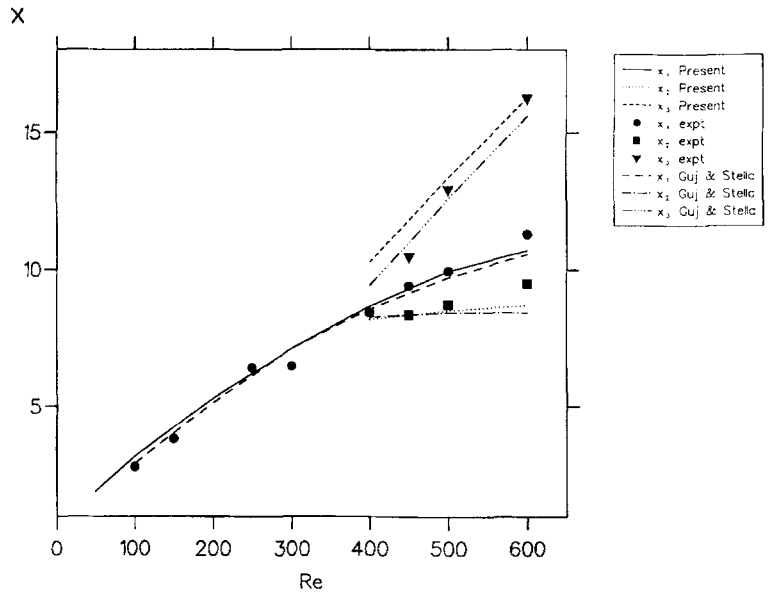

Figure 3. The variation of reattachment and separation lengths with Reynolds number

number flows the maximum pressure occurs on the lower boundary, downstream of the lower reattachment point. However, for high Reynolds numbers where an upper recirculation region occurs the location of the maximum pressure is downstream of the upper reattachment length on the upper boundary. The medium grids are sufficient for the QUICK, SOUBD and SOUD schemes to obtain values that are very similar in value. The hybrid scheme requires fine grids especially for the higher Reynolds number flows. This is demonstrated in Table IV which shows the maximum pressure coefficient for various grids for the $Re = 500$ case.

Finally, the numerical benchmark established at the Minisymposium on Outflow Boundary Conditions (MOBC) held at the University College of Swansea, U.K. in July 1989 is considered. The benchmark uses the present problem with a Reynolds number of $Re = 800$. The $Re = 800$ result has even longer reattachment and separation lengths which are probably sufficiently long to be seriously effected by the rather limited main channel length of 30 step-heights. Nevertheless, the various schemes are applied to grid 7 (200×100) as a comparison exercise with the MOBC benchmark. The hybrid scheme was the only scheme that successfully converged using grid 7, the results are shown in Table V. The source of instability was found to be the lack of grid refinement along the upper and lower solid boundaries. The results using a refined grid near the upper and lower boundaries are shown

Table IV. The maximum pressure coefficient for various grids $Re = 500$

grid	hybrid	central	QUICK	SOUBD	SOUD
1	0·378	—	0·428	0·451	0·430
2	0·462	—	0·468	0·468	0·468
3	0·480	—	0·470	0·470	0·470
4	0·499	—	0·475	0·476	0·475
5	0·491	—	0·475	0·476	0·475
6	0·486	0·468	0·474	0·475	0·475
7	0·483	0·474	0·475	0·476	0·476
8	0·480				

Table V. Reattachment and separation lengths for $Re = 800$

	x_1	x_2	x_3
Sohn ($x_{max} = 30$)	11·50	9·40	18·80
Betts & Sayma ($x_{max} = 14$)	11·16–11·18	8·56–8·58	—
Betts & Sayma ($x_{max} = 30$)	11·21	8·40	20·86
Srinivasan & Rubin ($x_{max} = 14$)	12·30	10·18	—
Srinivasan & Rubin ($x_{max} = 30$)	12·44	10·25	20·44
Srinivasan & Rubin ($x_{max} = 60$)	12·44	10·18	20·50
Gartling (coarse) ($x_{max} = 60$)	11·62	9·58	20·96
Gartling (fine) ($x_{max} = 60$)	12·20	9·70	20·96
Present results ($x_{max} = 30$)			
hybrid (uniform)	10·82	8·45	18·91
hybrid (refined grid)	10·99	8·55	19·55
QUICK	12·20	9·64	22·01
SOUBD	12·17	9·61	22·07
SOUD	12·09	9·54	22·21

on Table V for the various schemes. The refined grid also uses 200×100 grid points (uniform in the x co-ordinate) the smallest cell height is $\Delta y = 5 \times 10^{-3}$ (non-dimensionalised with step-height) linearly increasing to cell heights of $\Delta y = 3{\cdot}5 \times 10^{-2}$. The differences between the hybrid scheme results using a refined or uniform grid are quite small. The central-differencing scheme failed to converge successfully even for the refined grid. The table also shows some other available results, this list is far from exhaustive but it gives a fair impression how the recirculation regions behave with various numerical approaches. Generally, x_1, grows in size with grid refinement. This can be concluded from the various results which use a relatively coarse grid Sohn[8], Betts and Sayma[23] and Gartling[24] (coarse grid). The MOBC benchmark was developed to test a variety of outlet boundary conditions. Clearly, the boundary conditions discussed in Sani and Gresho[23] are very effective and various channel lengths, x_{max}, give very similar results even if the outlet boundary condition intersects a recirculation region ($x_{max} = 14$). The outlet boundary condition used in the present study fails if the outlet boundary is near the upper reattachment, x_3, refer to Sani and Gresho[23] for further details. The Gartling (fine grid) results and the Srinivasan and Rubin[23] results are probably the most reliable results as a benchmark result. The biggest discrepancy between these two sets of results is the upper separation length x_2, which was also found to be very difficult to resolve in the present study with grid refinement. The results used for comparison are an average of these two sets of results; $x_1 \approx 12{\cdot}3$, $x_2 \approx 9.9$ and $x_3 \approx 20{\cdot}7$. The hybrid scheme appears to under-predict all the reattachment and separation lengths by about one step-height. The QUICK, SOUBD and SOUD schemes, however, give reasonable agreement with the Gartling and the Srinivasan and Rubin results for the reattachment length x_1 and separation length x_2, the QUICK scheme has the best agreement. However, these schemes appear to give poor agreement for the upper reattachment length x_3 which is about one step-height further downstream. The present predictions are most likely in error caused by the simple outlet condition used which tends to reduce the v-velocities near the outlet.

CONCLUDING REMARKS

It would appear that almost any differencing-scheme applied to medium or fine grids produce results similar to the anticipated grid-independent results for the majority of cases. In the case of high Reynolds number flows the hybrid scheme fails to give reliable results for medium grids and the

central differencing scheme will only converge for fine grids. The accuracy achieved by the central-differencing scheme (if it converges), QUICK, SOUBD and SOUD schemes is virtually identical for the problem studied. Other numerical studies of the QUICK scheme and the SOUD scheme tend to favour the latter scheme but in the present study there is relatively large physical viscosity as well as pressure gradient terms acting as source terms and the behavior of the QUICK, SOUBD and SOUD schemes is very similar. It is not possible to conclude which is the most accurate but they all perform remarkably better than the hybrid scheme. The SOUD scheme can use higher time step parameters compared with QUICK and SOUBD schemes confirming its general robustness.

When uniform grids are considered then central-differencing, QUICK, SOUBD and SOUD schemes can be described by a general formulation using a single parameter to obtain the various schemes. The coefficients in the formulation can be revised in such a way to avoid negative coefficients or coefficients that tend to zero, either of which will tend to produce divergence in the matrix solution procedure.

ACKNOWLEDGEMENTS

I thank Ms A. Field for commenting on the original manuscript and Dr I. M. Hall for valuable technical comments.

REFERENCES

1. B. F. Armaly, F. Durst, J. C. F. Pereira and B. Schonung, 'Experimental and theoretical investigation of backward-facing step flow', *J. Fluid Mech.*, **127**, 473–496 (1983).
2. I. E. Barton, 'Laminar flow past an enclosed and open backward-facing step', *Phys. Fluids*, **6**, 4054–4056 (1994).
3. J. Kim and P. Moin, 'Application of a fractional-step method to incompressible Navier-Stokes equations', *J. Comp. Phys.*, **59**, 308–323 (1985).
4. S. C. Caruso, J. H. Ferziger and J. Oliger, 'Adaptive grid techniques for elliptic fluid flow problems', AIAA 25th Aerospace Sciences Meeting, paper AIAA-86-0498, Reno, Nevada, 1986.
5. S. Thangam and D. D. Knight, 'Effect of stepheight on the separated flow past a backward facing step', *Phys. Fluids*, **A1**, 604–606 (1989).
6. A. K. Runchal, M. S. Anand and H. C. Mongia, 'An unconditionally-stable central-differencing scheme for high Reynolds number flows', AIAA 25th Aerospace Sciences Meeting, paper AIAA-87-0060, Reno, Nevada, 1987.
7. G. Guj and F. Stella, 'Numerical solutions of high-Re recirculating flows in vorticity-velocity form', *Int. j. numer. methods fluids*, **8**, 405–416, (1988).
8. J. L. Sohn, 'Evaluation of FIDAP on some classical laminar and turbulent benchmarks', *Int. j. numer. methods fluids*, **8**, 1469–1590 (1988).
9. S. Thangam and D. D. Knight, 'A computational scheme in generalized coordinates for viscous incompressible flows', *Computer and Fluids*, **18**, 317–327 (1990).
10. P. Orlandi, 'Vorticity-velocity formulation for high Re flows', *Computers and Fluids*, **15**, 137–149 (1987).
11. F. H. Harlow and J. E. Welch, 'Numerical calculation of time dependent viscous incompressible flow of fluid with free surface', *Phys. Fluids*, **8**, 2182–2189 (1965).
12. S. V. Patankar, *Numerical Heat Transfer and Fluid Flow*, Hemisphere, Washington D.C. (1980).
13. P. J. Roache, *Computational Fluid Dynamics*, Ch. 3, Hermosa Publishers (1982).
14. B. P. Leonard, 'A stable and accurate convective modelling procedure based on quadratic upstream interpolation', *Comp. Meth. Appl. Mech. Eng.*, **19**, 59–98 (1979).
15. M. K. Patel and N. C. Markatos, 'An evaluation of eight discretization schemes for two-dimensional convection-diffusion equations', *Int. j. numer. methods fluids*, **6**, 129–154 (1986).
16. A. Pollard and A. L. -W. Siu, 'The calculation of some laminar flows using various discretisation schemes', *Comp. Meth. Appl. Mech. Eng.*, **35**, 293–313 (1982).
17. W. Shyy, S. S. Tong and S. M. Correa, 'Numerical recirculating flow calculation using a body-fitted coordinate system', *Numer. Heat Trans.*, **8**, 99–113 (1985).
18. W. Shyy, 'a study of finite difference approximations to steady-state, convection-domainated flow problems', *J. Comp. Phys.*, **57**, 415–438 (1985).
19. M. A. R. Sharif and A. A. Busnaina, 'Assessment of finite difference approximations for the advection terms in the simulation of practical flow problems', *J. Comp. Phys.*, **74**, 143–176 (1988).
20. C. A. J. Fletcher, *Comutational Techniques for Fluid Dynamics*, vol. II, ch. 17, Springer-Verlag (1988).
21. D. B. Spalding, 'A novel finite difference formulation for differential expressions involving both first and second derivatives', *Int. j. numer. methods eng.*, **4**, 551–559 (1972).

22. G. D. Raithby and G. E. Schneider, 'Numerical solution of problems in incompressible fluid flow: Treatment of the velocity-pressure coupling', *Numer. Heat Trans.*, **2**, 417–440 (1979).
23. R. L. Sani and P. M. Gresho, 'Résumé and remarks on the open boundary condition minisymposium', *Int. j. numer. methods fluids*, **18**, 983–1008 (1994).
24. D. K. Gartling, 'A test problem for outflow boundary conditions-flow over a backward-facing step', *Int. j. numer. methods fluids*, **11**, 953–967 (1990).